A Downlink Non Orthogonal Multiple Access for Chirp Spread Spectrum Communications

Guillaume FERRÉ[1], Baptiste LAPORTE-FAURET[1,2] and Mohamed Amine BEN TEMIM[1]
[1]Univ. Bordeaux, CNRS, Bordeaux INP, IMS, UMR 5218, F-33400, Talence, France
[2]THALES, France
Email: forename.name@{ims-bordeaux.fr[1], thalesgroup.com[2]}

***Abstract*—In this paper, we aim to enhance the spectral efficiency of Chirp Spread Spectrum (CSS) communications by transmitting simultaneously and on the same bandwidth several non orthogonal signals. Each receiver is able to demodulate its information taking advantage of a controlled time desynchronization between transmitted signals and/or an amplification diversity coupled with a successive interference cancellation algorithm. Various simulation results demonstrate the relevance of our proposition to decode multiple superposed CSS signals in a downlink situation.**

***Index Terms*—NOMA, Chirp Spread Spectrum, Successive Interference Cancellation, LoRa, IoT**

I. INTRODUCTION

In multiple access communication systems, it is paramount for the different users to be orthogonalized in order to avoid interference. Thus, several technics exist to access to the propagation channel. However, in a context of saturated frequency bandwidth, it can sometimes be difficult to provide a correct access for all users. Given the popularity of some communication systems, this phenomenon becomes more and more present. This is for instance the case in low power wide area network (LPWAN) communication systems which operate in free bands like industrial, scientific and medical (ISM) ones. Indeed, the exponential rise of connected devices using these particular frequency bands leads to an increase of the interference issues and, as a result, in the possible packet loss. More precisely, this is the consequence of the random access used by connected devices to send messages to the gateway. Indeed, in most situations, in order to minimize the energy consumption, a device will send its message whenever it wants without any concern regarding its environment i.e. without listening before talking as an instance. In order to avoid the loss of packets, several methods can be applied. First of all, on the level 2 protocol side (MAC layer), it is recommended to use time and frequency diversity by allowing the connected device to send back the information multiple times to receive an acknowledgment (ACK) from the gateway [1], [2]. This attempt is performed within the limit of the duty cycle or to prevent the network congestion. On the physical (PHY) layer side, recent works proposed:

1) To take advantage of the cooperation between gateways in order to reduce the packets loss,
2) To implement successive interference cancellation algorithms [3] to deal with these collisions and retrieve all the signals.

978-1-7281-8903-1/20/$31.00 ©2020 IEEE

These PHY layer proposals can be difficult to implement but provide huge advantages regarding the spectral efficiency since the nodes do not need to send back the information multiple times which is not the case for the MAC layer solution. The solution presented in [4] is also worth noticing since it proposes to divide the frequency band in two parts in order to allow the simultaneously transmission of two users but still at the expense of spectral efficiency. This idea of simultaneous transmission to reduce the packet loss was also studied by [5] which provided some feasibility insights by using slope-opposite chirps.

The majority of the above works were focused on uplink communications. However, the collision and congestion issues exist in both ways: uplink and also downlink. In this paper, we aim to propose to enhance the spectral efficiency of downlink transmission by allowing the simultaneous transmission of multiple packets on the same bandwidth when CSS communication is used. Indeed, we propose to control the time desynchronization of the superposed signals and to allocate different powers to the transmitted packets. The implementation of this solution is helped by the fact that the transmitted signals are received in phase. Based on the fast Fourier transform (FFT) size used to demodulate the CSS signals, we show that our proposition is naturally able to demodulate the interfering signals without any additional processing. If this is not the case, we propose to apply an interference cancellation algorithm coupled with a power allocation. Thus, this solution extend our previous work proposed in [6] for an uplink scenario. Indeed, if the gateway is able to effectively process multiple superposed signals with the same Spreading Factor (SF), then it would require to send multiple and superposed acknowledgments in order to comply with the transmission protocol such as LoRaWAN [7]. Thereby, the connected devices also need to be able to demodulate packets that can be in collisions. The relevance of our approach is demonstrated by simulations results in various scenarios when 2 packets are simultaneously transmitted.

The paper is organized as follows. In section II, we present our system model. Then, in section III, we describe the proposed algorithms used in order to allow each receiver to

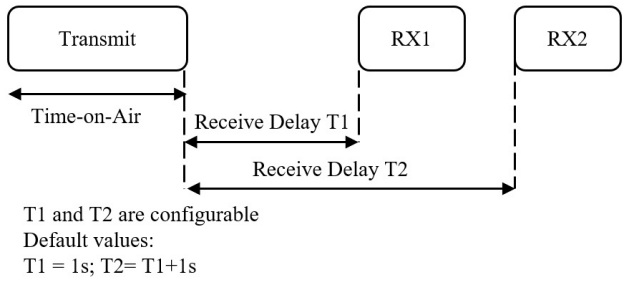

Fig. 1: Receive Windows - Class A LoRaWAN

process multiple superposed signals and decode the information. Simulation results are provided in section IV while section V presents the conclusion and future prospects.

II. System model

We consider a downlink communication system where several CSS signals are simultaneously transmitted on the same channel and with the same symbol time T. As an example, this situation can happen if the gateway receives in uplink several superposed signals and is able to decode all of them thanks to a dedicated algorithm such as the one presented in [3]. Indeed, the acknowledgment will be expected by each node on a similar time window. In this case, there is no orthogonal property between those signals. More precisely, the reception of a signal in the downlink case depends on level 2 protocol (MAC layer) for some energy consumption issues. Thus, if we consider a LoRa communications using LoRaWAN, the spectrum listening depends on the chosen communication class at the node level: A, B or C. In Class A, after sending messages, nodes expect an ACK from the network server during two pre-agreed time-slots known as "receive windows (RW)". Figure 1 depicts the RWs of Class A operating mode. Frequency and data rate of the first RW is the same as the uplink transmission parameters whereas the second slot operates on pre-agreed parameters to improve the robustness of message transmissions.

As presented in [8], receiving simultaneously two ore more signals with the same symbol time leads to a loss of orthogonality and may cause the destruction of all the packets. In the following, we recall the CSS PHY layer principle. Then we express the construction of the signal that we propose to send in order to be able to decode the simultaneous reception of two interfering signals. For more information about the CSS modulation and demodulation principle, the reader is invited to read [8].

A. Chirp modulation principle

The principle behind a linear CSS modulation lies in a base signal named as a chirp. This chirp frequency varies linearly from an initial frequency f_i to a final frequency f_f during the time symbol T. If we note $B = |f_i - f_f|$, then B corresponds to the signal bandwidth. When $f_i > f_f$, the chirp is considered as down-chirp while it is considered an up-chirp otherwise. Then, the chirp can be seen as a signal

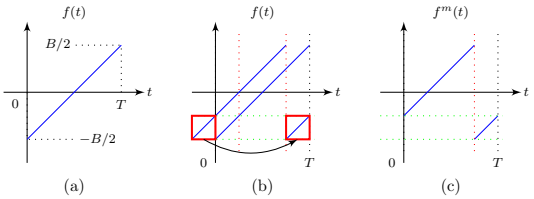

Fig. 2: Symbol → chirp association process - (a) up raw chirp - (b) process principle - (c) associated chirp.

which browse a time/frequency surface of $T \times B$. If we denote SF the number of bits/symbol, then we can associate to the $M = 2^{SF}$ constellation symbols, M chirp trajectories of T duration. SF also stands for spreading factor following the relation:

$$B \times T = 2^{SF} \tag{1}$$

The different trajectories are obtained by performing modulo T operations of the base chirp. If we denote $f(t)$ the base chirp defined for $t \in [0,T)$, then the chirp associated to the mth constellation symbol can be defined as:

$$\forall t \in [0,T),\ f^m(t) = f((t+\tau_m) \mod T) \tag{2}$$

where τ_m is obtained from an unique combination of SF bits. In the following, we consider that $\tau_m = \frac{mT}{M}$ given that m is obtained by gray coding of SF bits. Thereby, the complex envelope of a CSS signal for the transmission of a random binary information stream is a succession of random trajectories of chirps. If we denote $f_k(t-kT)$, the random signal transmitted during the time period $[kT,(k+1)T)$, then $f_k(t)$ is uniformly distributed in the set $\{f^0(t), \ldots, f^m(t), \ldots f^{M-1}(t)\}$. Fig. 2 provides an illustration of the different trajectory generation process.

B. Considered communication scenario

We consider a downlink communication system composed of two LoRa nodes and one gateway. If we note $s_1(t)$ and $s_2(t)$ the complex envelope of the payload transmitted by the gateway to the first and second LoRa node, respectively, the transmitted signal is expressed as follows:

$$s(t) = \sqrt{P_1} s_1(t) + \sqrt{P_2} s_2(t - \delta t_{1,2}) \tag{3}$$

Where $\delta t_{1,2} \in [0,T)$ corresponds to the time desynchronization between the nodes 1 and 2, and P_i is the power allocated to the ith node. We also define:

$$s_i(t) = \sum_{k=0}^{K_i - 1} e^{j\phi_{k,i}(t-kT)} \mathbb{1}_{[kT,(p+1)T)}(t) \text{ with } i \in \{1,2\} \tag{4}$$

Where K_i is the number of transmitted chirps. We note $f_{k,i}(t)$ the kth modulated chirp intented to the ith node. It can be expressed as the derivative of its phase $\phi_{k,i}(t)$:

$$f_{k,i}(t) = \frac{1}{2\pi} \frac{\mathrm{d}\phi_{k,i}(t)}{\mathrm{d}t} \tag{5}$$

Therefore, we obtain for $t \in [0, T - \gamma_i(k))$:

$$\phi_{k,i}(t) = 2\pi \left[\frac{B}{2T} t^2 + \left(\frac{m_i(k)}{M} - \frac{1}{2} \right) Bt \right] \tag{6}$$

And for $t \in [T-\gamma_i(k), T)$:

$$\phi_{k,i}(t) = 2\pi \left[\frac{B}{2T} t^2 + \left(\frac{m_i(k)}{M} - \frac{3}{2} \right) Bt \right] \quad (7)$$

where $\gamma_i(k) = \frac{m_i(k)}{B}$, with $m_i(k) \in \{0,...,M-1\}$ is the kth transmitted symbol intended to the ith node.

In order for the receiver to detect and synchronize on $s(t)$, we propose that node 1 and 2 share the same preamble. Thus, a preamble signal $s_{train}(t)$ of duration T_t similar for both nodes is added. Finally, the signal transmitted by the gateway can be expressed as:

$$x(t) = \sqrt{P} s_{train}(t) + s(t - T_t) \quad (8)$$

with $P = P_1 + P_2$.

C. Received signals

We consider a communication through a non-frequency selective channel with complex-valued channel gain $h_i \in \mathbb{C}$. The received signal on the ith node, sampled at $T_s = \frac{1}{uB}$ $(u \geq 1)$, is given by:

$$r_i(n) = h_i \times x(n - \Delta n_i) e^{j2\pi n T_s \Delta f_i + j\theta_i} + w_i(n) \quad (9)$$

Where $w_i(n) \sim \mathcal{N}_{\mathbb{C}}(0, \sigma_w^2)$ is the additive white Gaussian noise (AWGN). Δn_i and Δf_i stand for the time and frequency desynchronization respectively while θ_i represents the initial phase. Without loss of generality, we can consider in the following $h_i = 1$.

To detect the reception of LoRa-like signals, the receiver has to be in a listening mode. A step by step method to detect and synchronize LoRa-like signal is described in [9]. It should be noted that the method is based on the patent [10] written by the LoRa inventors.

Once synchronized[1], the CSS demodulator needs to perform a de-chirping operation such as explained in [11]. Then, it needs to estimate the most likely symbol by looking for the index $j \in \{0, \dots, M-1\}$ which maximize a FFT absolute value. However, given the proposed communication strategy, some additional processing must be implemented so that the nodes can correctly demodulate all the superposed signals sent by the gateway. In the next section, we propose an original way to perform the demodulation of two interfering LoRa-like signals.

III. Proposed receiver

Without loss of generality, we propose to develop the receiver equations for the simultaneous reception of two packets to nodes 1 and 2. The processing limits of more than two users are not the subject of this paper and will be studied in a future contribution.

The synchronization of nodes 1 and 2 will be performed in a similar way since they both share the same training message $s_{train}(t)$. Nevertheless, as their intended information are transmitted in a non-orthogonal way, each node needs to find its own data by removing the inter symbol interference (ISI) or by using the time delay introduced by the gateway to synchronize alternatively on both nodes without interference. We consider that one bit of control is dedicated to the identification of the node. Then, the node will know on which signal it needs to synchronize and decode the information. Thereafter, we detail the processing on the node level and the requirements of the transmitted signal.

[1]The goal of this paper is not to propose a novel way to synchronize in time and frequency the CSS signals. To that end, for our simulation results we use solutions proposed in [9].

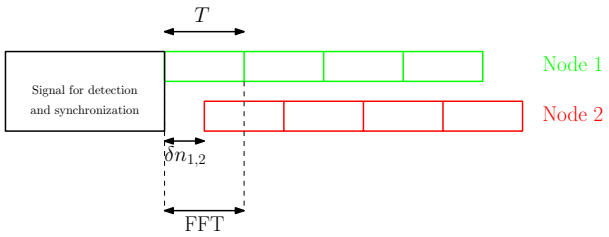

Fig. 3: LoRa-Like symbol detection principle when $\delta n_{1,2} = M/2$

After synchronizations, the received signal for each node, sampled at $T_s = 1/B$, can then be written as follows:

$$y_1(n) = \sqrt{P_1} s_1(n) + \sqrt{P_2} s_2(n - \delta n_{1,2}) + w_1(n) \quad (10)$$

$$y_2(n) = \sqrt{P_1} s_1(n + \delta n_{1,2}) + \sqrt{P_2} s_2(n) + w_2(n) \quad (11)$$

With $\delta n_{1,2} = \frac{\delta t_{1,2}}{T_s} \in \{0,...,M-1\}$.

Then, the processing of CSS signal is composed of two main steps: 1) dechirping, which consists in multiplying the received signals by a sequence of down-chirp signals, 2) symbol estimation based on FFT processing.

Thus, the signal obtained after the FFT and which corresponds to the processing of pth symbol of node 1 is equal to:

$$Y_1(k,p) = \frac{1}{\sqrt{M}} \sum_{n=0}^{M-1} \underbrace{(y_1(n,p) x_{ref}^*(n))}_{z_1(n,p)} e^{-j2\pi \frac{nk}{M}} \quad (12)$$

where $y_1(n,p) = y_1(n + pM)$ and $x_{ref}(n) = e^{j2\pi \left(\frac{1}{2M} n^2 - \frac{1}{2} n \right)}$ $\forall n \in [0,...,M-1]$. Based on [12] and after some calculations:

$$\begin{aligned} z_1(n,p) = & \sqrt{P_1} e^{j2\pi \frac{n m_1(p)}{M}} \\ & + \sqrt{P_2} e^{j2\pi \frac{n \bar{m}_2(p-1)}{M}} \mathbb{1}_{[0, \delta n_{1,2}-1]}(n) \\ & + \sqrt{P_2} e^{j2\pi \frac{n \bar{m}_2(p)}{M}} \mathbb{1}_{[\delta n_{1,2}, M-1]}(n) + \tilde{w}_1(n) \end{aligned} \quad (13)$$

Where $\mathbb{1}_{[0,x)}(t)$ stands for the indicator function, and with

$$m_2(p) = (\delta n_{1,2} + \bar{m}_2(p)) \mod M \quad (14)$$

and

$$m_2(p-1) = (\delta n_{1,2} + \bar{m}_2(p-1)) \mod M \quad (15)$$

Based on (13), $Y_1(k,p)$ can be written as follows:

$$\begin{aligned} Y_1(k,p) = & \sqrt{P_1 M} \delta(k - m_1(p)) + Y_{1,p-1}(k,p) \\ & + Y_{1,p}(k,p) + \tilde{W}_1(k) \end{aligned} \quad (16)$$

Where $\tilde{W}_1(k) \sim \mathcal{N}_{\mathbb{C}}(0, \sigma_w^2)$ is the FFT of the noise $\tilde{w}_1(n)$ and $Y_{1,p}(k,p)$ represents the FFT of the part of the chirp transmitted by node 2 and associated to the pth symbol $m_2(p)$.

After some manipulations it is straightforward to demonstrate that:

$$Y_{1,p-1}(k,p) = \sqrt{\frac{P_2}{M}} e^{\theta_{p-1}} \delta n_{1,2} \frac{sinc(\pi \frac{\bar{m}_2(p-1)-k}{M} \delta n_{1,2})}{sinc(\pi \frac{\bar{m}_2(p-1)-k}{M})} \tag{17}$$

and

$$Y_{1,p}(k,p) = \sqrt{\frac{P_2}{M}} e^{\theta_p} (M - \delta n_{1,2}) \frac{sinc(\pi \frac{\bar{m}_2(p)-k}{M} (M - \delta n_{1,2}))}{sinc(\pi \frac{\bar{m}_2(p)-k}{M})} \tag{18}$$

The two cardinal sines (17) and (18) represent the ISI from node 2 on node 1. It should be noted that since the arguments θ_p and θ_{p-1} are unnecessary in the following, they are not developed. A similar development can be achieved for $y_2(t)$.

In order for nodes to be able to demodulate the symbols intended for them, it is necessary to minimize or even eliminate the ISI. Thus, we propose two strategies:

1) The first strategy is to transmit the signals with the same power, $P_1 = P_2$ and to desynchronize them temporally by $\delta t_{1,2} = T/2$. Indeed, we can see from (17) and (18) that for $\delta n_{1,2} = \frac{M}{2}$, both cardinal sines peaks have the same power which corresponds to half the initial power i.e. a 6 dB loss. As a result, if $s_1(t)$ and $s_2(t)$ are delayed by $\delta t_{1,2} = \frac{T}{2}$ the power diversity gain is maximized. This result is interesting since we could transmit both signals at the same power on the gateway side and use only the time delay $\delta t_{1,2}$ to create a power diversity. Thus, this parameter would seem enough to directly demodulate the signal of interest without the needs to perform an interference cancellation. Fig. 4 shows the frequency representation of the received signals when a perfect synchronization on node 1 is assumed. We can clearly notice the two cardinal sines for the node 2 and the Dirac comb for the node 1. We can also see that, when $\delta t_{1,2} = T/2$, the power diversity on the spectrum is maximized and that the two cardinal sines are lowered at the same level.
2) The second strategy involves allocating different powers and implementing a successive interference cancellation (SIC) algorithm. Indeed, for a low value of SF, the power ratio obtained by setting $\delta t_{1,2} = T/2$ is not sufficient to limit the effect of the ISI. We then propose to allocate more power to a node. Thus, we limit the effect of the ISI on this node. Its demodulation is thus facilitated making it possible to cancel its contribution in the received signal.
   More precisely, when the interference cancellation is implemented, we consider the power ratio between the two nodes as follows: $PR = 10\log_{10}(\frac{P_1}{P_2}) \geq 0$ dB. In this case node 2 has to cancel the contribution of node 1 before starting the decoding process of its frame. To this end, after the synchronization to the beginning of the payload of node 1, node 2 estimates, in each T-long sequence, the frequency, the magnitude and the phase of the main peak in the FFT. Then, it reconstructs the information of node 1 and removes it from the synchronized dechirped signal. For more details on the SIC algorithm, reader can refer to [3]. After canceling the contribution of node 1, node 2 can identify easily the start of its frame by knowing the time delay $\delta n_{1,2}$.

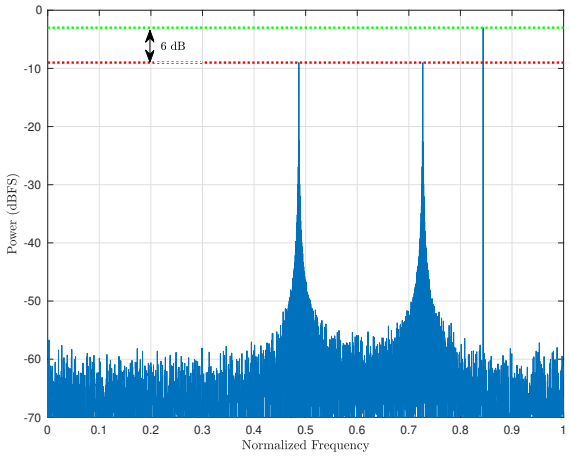

Fig. 4: Observation used to demodulate a symbol when $\delta n_{1,2} = M/2$ and $SF = 12$

In the next section, we present some simulation results in order to study the relevance and the performance of our proposed solution.

IV. Results

The simulation results we present are obtained from a LoRa signal simulator that we developed in MATLAB. Thus, we simulate the interleaving and de-interleaving blocks, but also the channel coding/decoding parts, recalled hereafter.

A. Channel coding and interleaving in LoRa

In order to increase the robustness of LoRa modulation against interfering bursts and off-by-one errors, bits are encoded before the chirp generation. The encoding stages are as follows:

1) Interleaving: Interleaving is a process that scrambles data bits throughout the packet. It is often combined with forward error correction (FEC) to make the data more resilient to bursts of interference [13]. According to the patent [10], diagonal interleaver is implemented in LoRa chips.

2) Forward error correction: FEC is used for controlling errors in data transmission over unreliable or noisy communication channels. In LoRa, Hamming FEC is used with a variable codeword size ranging from 5 to 8 bits [10]. Furthermore, the data size per codeword is set to 4 bits, which allow to define the coding rate as $\frac{4}{4+CR}$, with $CR \in \{1,...4\}$ is the code rate or also the number of redundancy bits.

B. Simulation results

In the following, the used signal to noise ratio (SNR) is defined for the ith node as SNR=P_i/σ_w^2. In addition, when

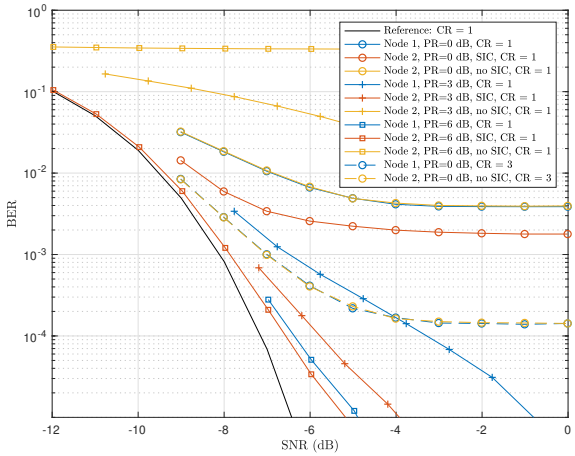

Fig. 5: BER curves for node 1 and 2, $SF = 7$ and perfect time/frequency synchronizations

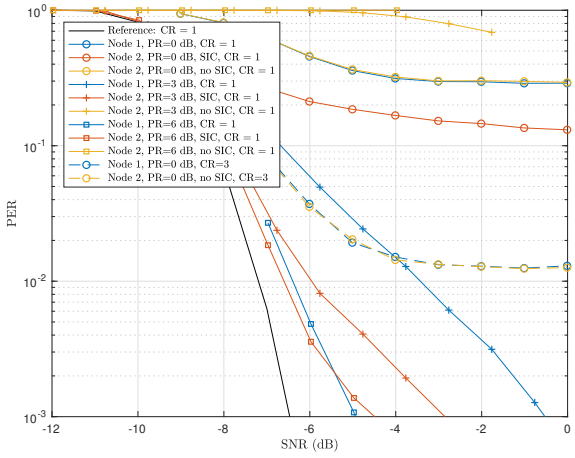

Fig. 6: PER curves for node 1 and 2, $SF = 7$ and perfect time/frequency synchronizations

time and frequency synchronization are performed, Δf_i and Δn_i are uniformly distributed in $\pm\frac{B}{4}$ and $\pm 10T$, respectively.

a) Impact of the Power Ratio and the SIC: We first consider the case of $SF = 7$ and study the decoding performance for different power ratio with or without the SIC algorithm.

We can see in Fig. 5 the bit error rate (BER) evolution when perfect time and frequency synchronizations are considered. We can notice that the performance depends on the power ratio fixed between the two nodes at the gateway. Combined with the time delay $\delta t_{1,2} = T/2$ which creates another power diversity, we are able to perform the interference cancellation under certain conditions. Indeed, we can see that the best results are obtained for a larger PR i.e. PR=6 dB in our case. With $\delta t_{1,2} = T/2$, it means there is a gap of 12 dB between the peaks in FFT module which is enough to properly demodulate the first signal, to remove its contribution and to

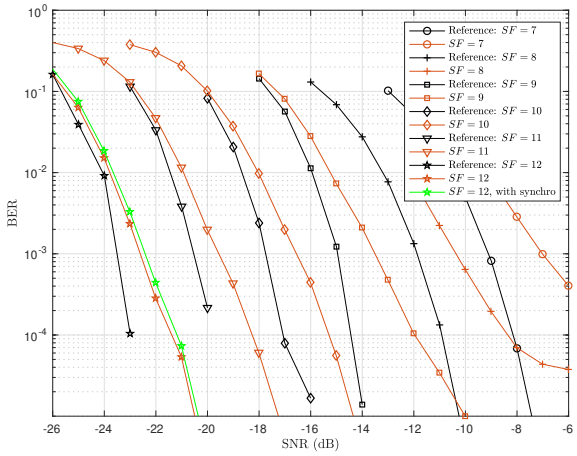

Fig. 7: BER curves for node 2, different SFs, CR = 3, no SIC (PR=0 dB) and perfect time/frequency synchronizations unless stated otherwise

demodulate the other node. The decoding performance of node 2 are slightly degraded for a lower PR, as it can be seen when PR=3 dB. Indeed, for a BER=10^{-4}, compare to the reference performance (i.e the BER evolution without interference on AWGN channel) we have a loss of 0.6 dB for PR=6 dB whereas 1.3 dB are lost for PR=3 dB. In addition, we can see that for PR=0 dB (i.e. by only using the diversity introduced by $\delta t_{1,2}$), the SIC algorithm does not work properly since it appears there is not enough margin between the peak to properly demodulate the signals. We also represent the packet error rate (PER) results in Fig. 6 for packet length of 55 bytes.

We can notice that the results for PR=0 dB are close with or without SIC. Even though the performance are not completely satisfactory, we can see the BER floor can be reduced by enhancing the coding rate at CR = 3.

In the following paragraph, we propose to analyze the impact of SF and the coding rate on the performance of our proposal.

b) Impact of the SF and the coding rate: We now only consider the case of PR=0 dB i.e. by only using the power diversity introduced by the time delay $\delta t_{1,2}$ and study the impact of the SF when CR = 3. In Fig. 7, we can see that the SF has a direct impact on the decoding performance without using a SIC algorithm. Indeed, the greater the SF is, the lower is the BER floor. Moreover, although we saw in Fig. 5 that a coding rate increase enhances the performance for $SF = 7$, we can see here that the coding rate has a greater impact for larger SFs with performance close to the reference curve for $SF > 8$. In addition, we can see for $SF = 12$ that the performance remain excellent even when we activate the time and frequency synchronization algorithms. This fact is also confirmed by Fig. 8 which represents the BER performance only for $SF = 12$. We can see that, for this high SF, the SIC at PR=6 dB is much less necessary compared to no SIC at PR=0 dB whether for CR = 1 and especially for CR = 3

TABLE I: Node 2, PER=10^{-2}, CR = 3. Deviation from the reference curve (dB). Packet length of 55 bytes

Parameters / SF	Perfect synchronization		With synchronization ($u=10$)	
	SIC, PR=6 dB	no SIC, PR=0 dB	SIC, PR=6 dB	no SIC, PR=0 dB
7	0.8	∞	0.8	∞
8	0.7	2.4	0.7	2.5
9	0.6	1.7	0.7	1.7
10	0.5	1.5	0.6	1.7
11	0.4	1.2	0.5	1.4
12	0.2	0.9	0.3	1.1

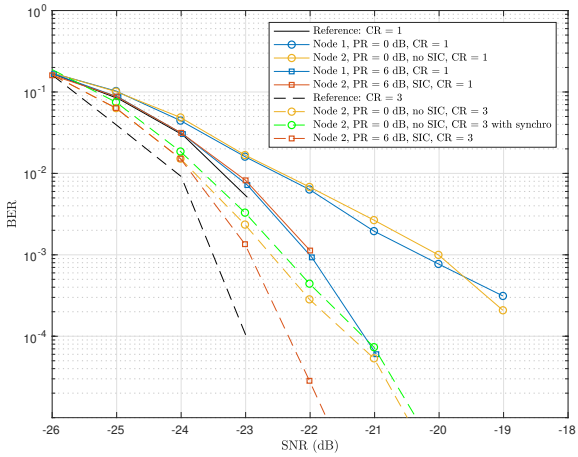

Fig. 8: BER curves for node 1 and 2, $SF = 12$ and perfect time/frequency synchronizations unless stated otherwise

which was not the case in Fig. 5 for a low $SF=7$.

It is also interesting to compare the results without SIC to the ones obtained with SIC and PR=6 dB. Due to the lack of space, we chose to present them through PER results in Table I. We can see that these results confirm our first observation: The SIC with PR=6 dB can be interesting for low SFs such as $SF = 7$ and $SF = 8$ with a deviation even at ∞ for $SF=7$ due to the PER floor. However, when we reach greater SFs, the SIC is no longer competitive since the results are close to the ones with no SIC at PR=0 dB. Moreover, we can see that the synchronization is well performed and does not degrade too much the performance. These results show that we are able, for certain SF ($SF>8$), to properly decode the information of both nodes without interference cancellation with an appropriated coding rate. For lower SFs ($SF=7$ and $SF=8$), we need to add more power diversity at the gateway and so need to perform a SIC algorithm at the receiver side.

V. Conclusion

In this paper, we extended a previous solution to receive and decode multiple superposed CSS signals on the same SF in an uplink communication to a downlink situation. In the case of two users, we showed that we were able to adapt our previous interference cancellation algorithms to this specific case by using power diversity at the gateway and by introducing a time delay so that the received power are optimized to perform the demodulation. Moreover, we showed that a power diversity at the transmitter was not necessary and that the SIC was not necessarily needed when the signals are sent at the same power. This solution was validated through simulations which tend to show that this method can be applied in existing IoT networks and thus enhance the spectral efficiency.

As future prospects, we plan to propose an optimization of the power diversity distribution by using the received SNR for the uplink communication and to analyze the capacity of the receiver to process more than two users.

References

[1] LoRa Alliance, "LoRaWAN® Specification v1.1," 2017. [Online]. Available: https://lora-alliance.org/resource-hub/lorawanr-specification-v11

[2] Sigfox, "Sigfox - The Global Communications Service Provider for the Internet of Things (IoT)," 2018. [Online]. Available: https://www.sigfox.com/en

[3] B. Laporte-Fauret, M. A. Ben Temim, G. Ferre, D. Dallet, B. Minger, and L. Fuché, "An enhanced lora-like receiver for the simultaneous reception of two interfering signals," in *2019 IEEE 30th Annual International Symposium on Personal, Indoor and Mobile Radio Communications (PIMRC)*, 2019, pp. 1–6.

[4] L. Vangelista and A. Cattapan, "A new lora-compatible modulation improving the lorawan network level performance," in *2019 IEEE Latin-American Conference on Communications (LATINCOM)*, 2019, pp. 1–6.

[5] L. Vangelista and A. Cattapan, "Extending the lora modulation to add further parallel channels and improve the lorawan network performance," 2020.

[6] M. A. B. Temim, G. Ferré, B. Laporte-Fauret, D. Dallet, B. Minger, and L. Fuché, "An enhanced receiver to decode superposed lora-like signals," *IEEE Internet of Things Journal*, pp. 1–1, 2020.

[7] J. P. Shanmuga Sundaram, W. Du, and Z. Zhao, "A survey on lora networking: Research problems, current solutions, and open issues," *IEEE Communications Surveys Tutorials*, vol. 22, no. 1, pp. 371–388, 2020.

[8] M. Chiani and A. Elzanaty, "On the lora modulation for iot: Waveform properties and spectral analysis," *CoRR*, vol. abs/1906.04256, 2019. [Online]. Available: http://arxiv.org/abs/1906.04256

[9] C. Bernier, F. Dehmas, and N. Deparis, "Low complexity lora frame synchronization for ultra-low power software-defined radios," *IEEE Transactions on Communications*, pp. 1–1, 2020.

[10] O. Seller and N. Sornin, "Low power long range transmitter," Aug. 7 2014, uS Patent App. 14/170,170. [Online]. Available: http://www.google.com/patents/US20140219329

[11] G. Colavolpe, T. Foggi, M. Ricciulli, Y. Zanettini, and J. Mediano-Alameda, "Reception of lora signals from leo satellites," *IEEE Transactions on Aerospace and Electronic Systems*, pp. 1–1, 2019.

[12] G. Ferré and A. Giremus, "LoRa Physical Layer Principle and Performance Analysis," in *2018 25th IEEE International Conference on Electronics, Circuits and Systems (ICECS)*, Dec 2018, pp. 65–68.

[13] M. Knight and B. Seeber, "Decoding LoRa: Realizing a Modern LPWAN with SDR," *Proceedings of the GNU Radio Conference*, vol. 1, no. 1, 2016. [Online]. Available: https://pubs.gnuradio.org/index.php/grcon/article/view/8